

DESIGN AND ANALYSIS OF A BIONIC ADHESIVE FOOT FOR GECKO ROBOT CLIMBING THE CEILING

Zhiwei Yu,* Ye Shi,* Jiaxing Xie,* Simon X. Yang,** and Zhendong Dai*

Abstract

Most of geckos can climb the ceiling smooth surface easily. This amazing ability in locomotion of geckos depends on the plenty setae of gecko's foot. Some researchers found the structure function of gecko's setae and produce different dry adhesive materials. We selected the dry adhesive material, which had mushroom-shaped adhesive microstructure (MSAMS), and tried to apply it in climbing ceiling experiment of a bio-inspired gecko robot with four legs. In this paper, a novel bionic adhesive foot was designed by studying on the structures and locomotion of gecko's foot. To apply novel bionic adhesive foot in ceiling locomotion successfully, the mechanical property of MSAMS with different structures of gecko-inspired robot was tested and analyzed. We selected the optimal structures of gecko-inspired robot and applied it in the ceiling locomotion. Bio-inspired gecko robot with the novel adhesive foot climbed the ceiling smooth surface stably, and it showed the rationality and feasibility of the bionic foot structure design.

Key Words

Gecko robot, bionic adhesive foot, climbing the ceiling, dry adhesive materials

1. Introduction

We all know that many geckos can move freely on the horizontal, vertical and inverted smooth surfaces in 3-dimension space, whose amazing adhesive abilities depends on van der Waals forces, because there are the countless setae on the toes [1]–[4]. This dry adhesion method with van der Waals force will be better than wet, magnetic,

vacuum adhesion, because it does not need liquid in wet adhesion, magnetic material in magnetic adhesion and air pressure in vacuum adhesion. Dai developed several kinds of force sensors to measure three-dimensional contact forces of gecko and found the kinematics and dynamics of geckos on horizontal, vertical and ceiling locomotion [5]–[8]. After understanding the gecko adhesive abilities, many researchers began to create a gecko tape for climbing robot. Murphy produced several new fibre arrays whose tips had directional friction [9]. Das showed a sloped Polydimethylsiloxane (PDMS) and analyzed the friction of dry adhesive material on different surfaces [10]. Gorb produced the dry adhesive material with polyvinyl siloxane (PVS) and showed the geometry structure in [11].

Based on these relative researches, scientists designed different climbing robots such as the wheel-legged, pedrail and track-wheel robot. The climbing robot named Mini-WhegsTM applied PVS material and designed the wheel-leg to climb the vertical surface by a single motor [12]. Wu presented a pedrail climbing robot, which walked on a vertical surface with the PDMS material [13]. A climbing robot which tried to use dry adhesive material with elastomer was developed by Seo [14]. Koh presented a track-wheel climbing robot, which used a hybrid adhesive material [15]. In fact, these robots are not like gecko which has four legs. But, some of legged climbing robots cannot climb up to 90° vertical surface. Unver focused on the development of a gecko-inspired climbing robot, which can climb 85° sloped surfaces [16]. Birkmeyer presented a climbing hexapod equipped with a bio-inspired adhesion feet climbing the 70° sloped surfaces [17]. Although, Kim developed a new gecko climbing robot called Stickybot, which climbed on the vertical smooth surfaces by directional dry adhesive materials [18]. Yu designed a gecko robot and applied dry adhesive material with MSAMS. It can climb on the smooth vertical glass wall feasibly and stably [19], [20].

Some researchers presented novel robot which tried to climb the ceiling. Unver presented a simple and lightweight climbing robot using polyurethane, it had sixteen legs with elastomer adhesives on its palm, and passive peeling

* Institute of Bio-inspired Structure and Surface Engineering, College of Astronautics, Nanjing University of Aeronautics and Astronautics, China; e-mail: yuzhiwei@nuaa.edu.cn, {1967528445, 543668094}@qq.com, zddai@nuaa.edu.cn

** Advanced Robotics and Intelligent Systems (ARIS) Laboratory, School of Engineering, University of Guelph, Guelph, Ontario, Canada N1G 2W1; e-mail: syang@uoguelph.ca

Corresponding author: Zhiwei Yu

Recommended by Prof. Jason Gu

(DOI: 10.2316/Journal.206.2018.4.206-5412)

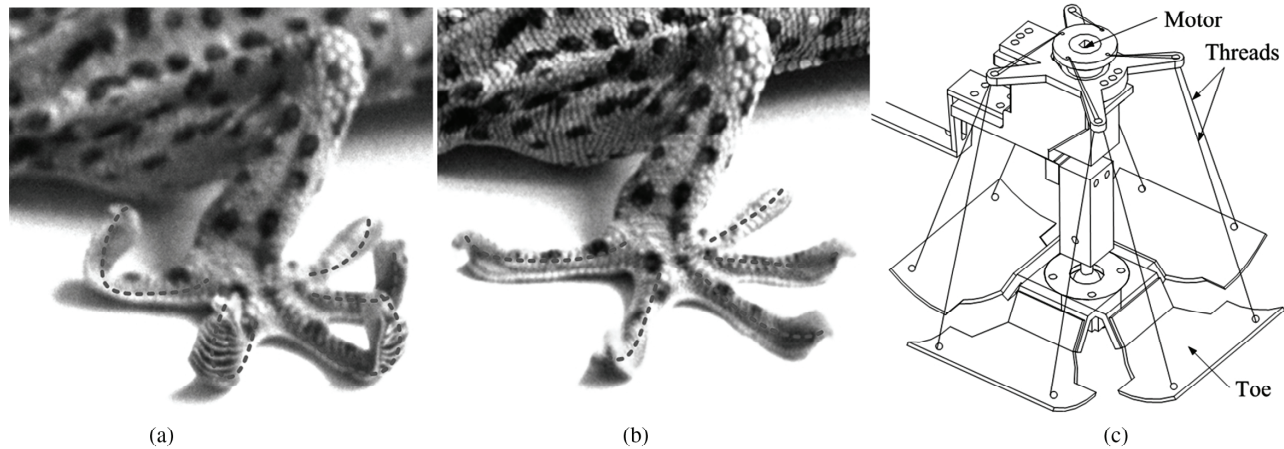


Figure 1. Design of the bionic gecko foot: (a) Eversion of gecko's toes; (b) stretching of gecko's toes; and (c) the structure of the bionic gecko foot.

mechanism was used to climb on inverted surface [21]. Unver also presented a wheeled Tankbot with elastomer adhesive tread with payload (40 g) on inverted surfaces, and series of Tankbot IV and V were driven by the same adhesive tread [22], [23]. Breckwoldt designed a lightweight climbing robot with rotating wheel-leg, and it used MSAMS tape to walk on inverted glass ceilings [24]. Ko presented a quadruped robot walking on the ceiling with velocity (1 mm/s) by tripod gait. The robot used PDMS, and its each leg was driven by three motors. Therefore, the adhesive foot was passively peeled off by the leg, and it will increase energy consumption because big adhesive force will be needed in other feet [25].

Compared to gecko, current climbing robots cannot move like the gecko in locomotion. There is not a legged bionic gecko robot which can climb the ceiling like geckos similarly. In this paper, a novel legged gecko robot with 16 active DOF and 12 passive DOF was presented. It was mimicked the characteristics of geckos with tendons and had the adhesive abilities like geckos which can climb the ceiling surface using dry adhesive material with diagonal gait.

This paper was narrated by following sequences. Section 2 presented a bionic adhesive foot with dry adhesive material (PVS) and showed the methods and equipment in the testing experiment. Section 3 showed the testing results of mechanical properties. We discussed the testing results and guided the experiments of the bionic gecko foot in Section 4. The bionic gecko robot using dry adhesive material PVS can climb the inverted glass ceiling. Finally, the conclusions of the paper and future research works were reported.

2. The Development of Bionic Adhesive Foot

If a legged gecko robot climbs the ceiling surface well successfully, the normal adhesive forces are very important because of resisting the weight of robot in ceiling locomotion. Due to some dry adhesive materials have big tangential adhesive forces and small normal adhesive forces, it will be easy to design the adhesive foot for legged gecko robot

climbing the wall and hard to design the adhesive foot for legged gecko robot climbing the ceiling.

During a long time of feeding geckos, we have carried out to observe the locomotion of geckos on ceiling and wall and find the mode of the gecko's toes locomotion. As shown in Figure 1, the gecko's toes can be actively driven by its tendons. First, gecko's toes will be turned over by tendons before its foot contacts with a surface. After that, gecko's toes will stretch completely and keep the setae on the toes contacting with the surface well. As the same way, gecko's toes will be turned over again by tendons before the gecko's foot leaves the surface. Base on the locomotion mechanism of the gecko's toe, we design a novel bionic adhesive gecko foot with four toes, and each toe is connected with two threads which like gecko's tendons. Eight threads are driven by a motor, as shown in Figure 1(c).

We all know that the adhesive capacity of gecko is depended on the countless setae under the toes. Some researchers had developed some dry adhesive materials, such as PVS, PDMS and so on. The research team that led by professor Dai in the Institute of Bio-inspired Structure and Surface Engineering (IBSS) has cooperation research with professor Gorb, who had provided us the PVS for the climbing robot experiment. Gorb analyzed the different factors influencing adhesion forces under different situation [26]. The peel-off forces of MSAMS at different retraction speed was measured under different atmospheric pressures [27]. In this paper, we will apply the dry adhesive material (PVS) in our Bio-gecko robot.

We observed the micro-structure of dry adhesive material (PVS) by optical microscope and measured the geometry microstructure sizes. Figure 2(a) showed the geometry structures of the MSAMS. The diameter of mushroom-shaped pad was $40 \mu\text{m}$, and the distance between the two centres of mushroom-shaped structures was $60 \mu\text{m}$. The head of mushroom-shaped microstructures was like disc-shaped called adhesive unit (AU). After the observation of MSAMS, we designed a novel toe model with MSAMS showed in Fig. 2(b). The dry adhesive material included MSAMS and sticky glue which help to connect with a

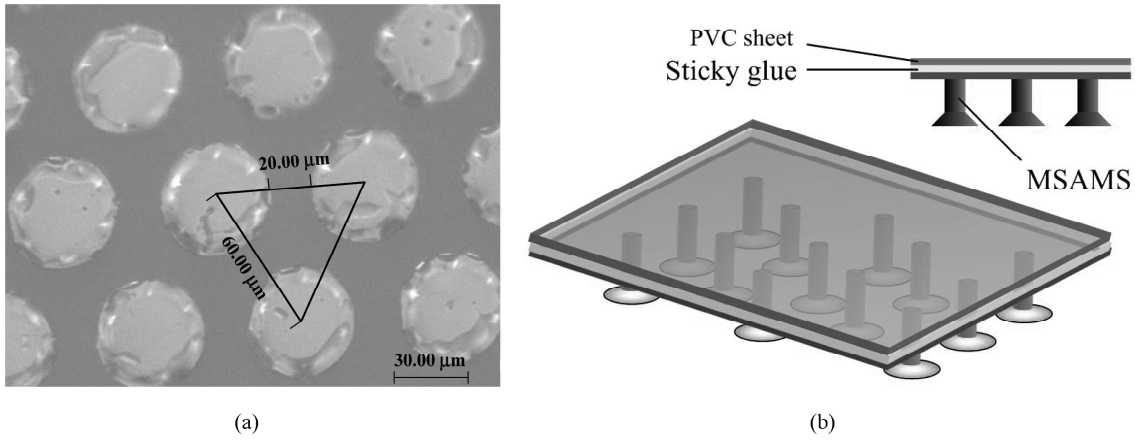


Figure 2. Dry adhesive material: (a) Geometry structures of MSAMS and (b) structure of bionic gecko's toe.

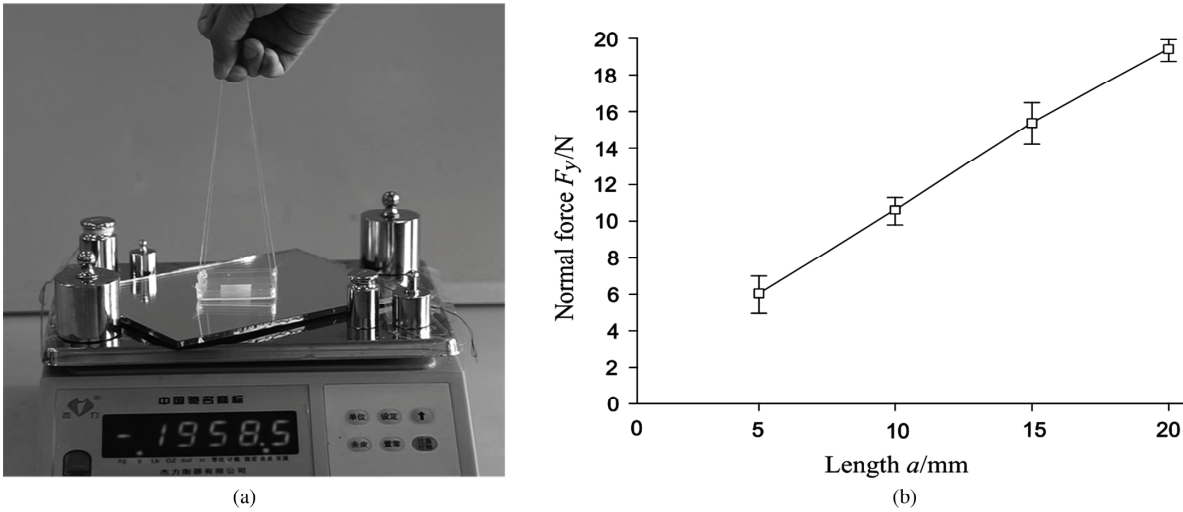


Figure 3. The experiment and results for testing the normal adhesive force: (a) The operation in normal force testing and (b) the normal forces under different contact areas.

polyvinyl chloride (PVC) sheet as the substrate of toe in gecko robot foot.

3. Test Methods and Results

As the structures of bionic adhesive gecko foot are showed, different thicknesses PVC sheets will influence the normal adhesive force of foot. We will analyze adhesion performance which was influenced by many more different factors. The testing experiments in this sequence: (1) the relationships between the sizes of contact areas and normal adhesive forces; (2) testing contact areas percentages with different thicknesses PVC sheets under a preload; and (3) the maximal normal adhesive force with different structures and locomotion of the toes.

3.1 Contact Areas and Normal Force

To test the maximal normal adhesive force under different contact areas, four sizes of $a \times b$ with 5 mm \times 20 mm, 10 mm \times 20 mm, 15 mm \times 20 mm and 20 mm \times 20 mm had been selected.

As shown in Fig. 3, we used an electronic scale to test the normal adhesive force of dry adhesive material.

Four 1-D force sensors were used, and the span of force sensor was about 10 kg weights. The error range of each force sensor was ± 0.1 g, and the data were showed on the screen. We keep the hard PVC sheet (5 mm thickness) with dry adhesive material contact with the mirror completely by manual operation. If the normal adhesive force was increasing at maximal value, the dry adhesive material may be separated with the mirror rapidly. Figure 3(a) showed the operation of experiment. We carried out the experiments more than seven times and got all the data by the camera. Figure 3(b) showed the average values of the maximal normal adhesive force were 6.4, 10.3, 15.2 and 19.5 N, when the length (a) equalled to 5, 10, 15 and 20 mm, respectively. It shows that normal adhesive force and size of contact areas have linearity relationship obviously.

3.2 Contact Areas Percentages with Different Thicknesses

We selected five pieces of dry adhesive material sample with the sizes of 10 mm \times 10 mm in testing of contact areas percentages with different thicknesses PVC sheets. Four kinds of different thicknesses PVC sheets were selected which may be designed as the substrate of toe in gecko

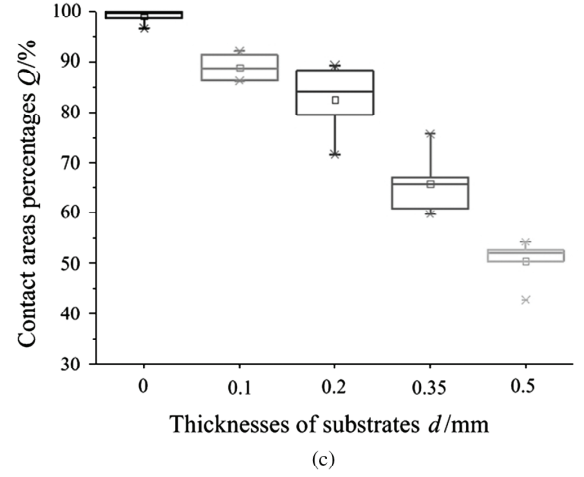
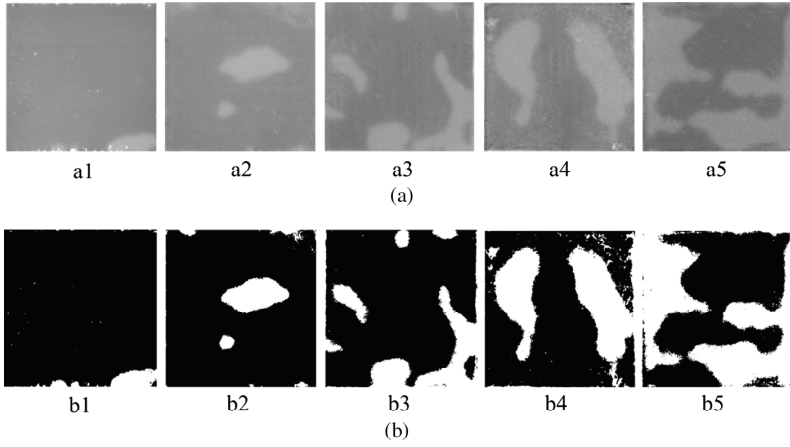


Figure 4. The experiment and results for testing contact areas percentages: (a) Contact areas; (b) contact areas after image binary progressing (a1 and b1, a2 and b2, a3 and b3, a4 and b4, a5 and b5 were 0, 0.1, 0.2, 0.35, 0.5 mm thicknesses of PVC sheets pictures, respectively); and (c) contact areas percentages with different thicknesses substrates.

robot, such as 0.1, 0.2, 0.35 and 0.5 mm. Five pieces of dry adhesive material sample will contact a smooth mirror. A normal force with preload (50 g) was put on the piece of dry adhesive material sample one by one. All the data had been tested five times during this testing experiment, and the pictures of contact areas were recorded by a camera.

Figure 4(a) showed some pictures of contact areas. Figure 4(b) showed the contact areas after image binary progressing, and contact areas percentages were easily calculated with pixel density. Figure 4(c) shows the contact areas percentages (Q) with different thicknesses (d) PVC sheets (0.1, 0.2, 0.35, 0.5 mm) under 50 g preload, and 0 mm thickness means there is no PVC sheet that was used. Therefore, each pieces sample of dry adhesive material was pressed with 4.9 KPa.

As shown in Fig. 4(c), under a constant preload (50 g), the contact areas percentages of dry adhesive materials will reduce by the increasing of thicknesses of PVC sheets. The sample with no PVC sheet contacted with the mirror completely, and average contact areas percentage was about 99.5%. But, the sample with 0.5 mm thickness PVC sheet cannot contact with the mirror well, its average contact areas percentage was about 52.5%. Therefore, we deduced that the soft substrate contributes to increase the contact areas and helps bio-gecko toes to contact with target surface completely.

3.3 Hypothetical Model of Adhesive Material with Different Thicknesses

We had discussed the peel-off force curves under different thickness of PVC sheets in [20]. The peel-off force when the angle (θ) changed from 0° to 13.0° was 40 times detachment force when the angle changed from 90° to 180° . The average value of the tangential force was 19.4 N under contact area ($20 \times 20 \text{ mm}$), and the tangential adhesive force and size of contact areas had linearity relationship obviously. So, it presented very different forces which appeared in one material.

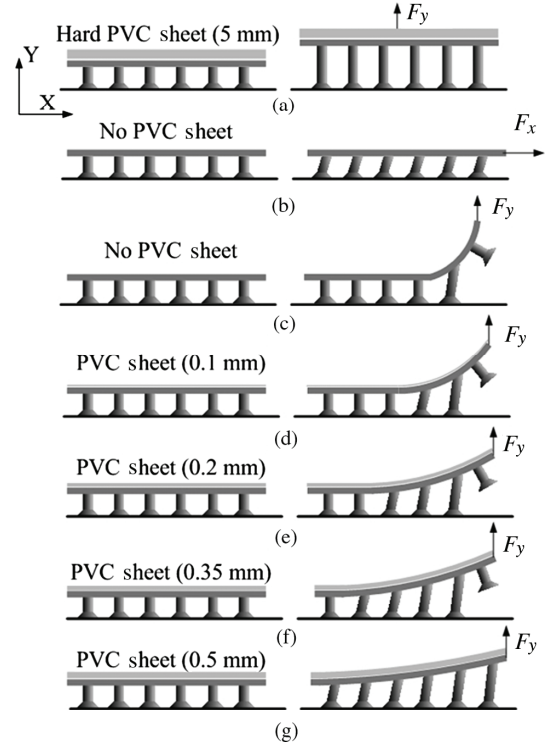


Figure 5. A model of adhesive material with different thicknesses substrate: (a) MSAMS with hard PVC sheet (5 mm) was acted by normal force (F_y); (b) MSAMS with no PVC sheet was acted by tangential force (F_x); (c) MSAMS with no PVC sheet was acted by normal force (F_y); (d) MSAMS with PVC sheet (0.1 mm) was acted by normal force (F_y); (e) MSAMS with PVC sheet (0.2 mm) was acted by normal force (F_y); (f) MSAMS with PVC sheet (0.35 mm) was acted by normal force (F_y); and (g) MSAMS with PVC sheet (0.5 mm) was acted by normal force (F_y).

We hypothesized a model of adhesive material with different thicknesses substrate as shown in Fig. 5, and all the head of mushroom-shaped microstructures called adhesive unit (AU) had a maximal adhesive force (F_{\max}).

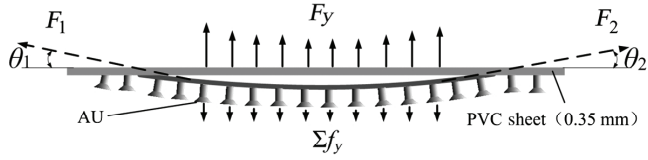


Figure 6. Design and analysis of a novel adhesive toe.

If external force is larger than maximal adhesive force (F_{\max}), then AU will separate with the mirror surface. We found that the peel-off normal force with hard backing material (5 mm thickness) was much larger than the force with 0.1, 0.2, 0.35 and 0.5 mm thickness PVC sheet which were flexible, because all AU presented in the maximal acting force effectively as shown in Fig. 5(a). In the same way, Fig. 5(b) showed that the peel-off tangential adhesive force (F_x) was also the largest along to axis x .

If the peel-off adhesive force was acted one side of PVC sheets, peel-off normal adhesive force with 0.5 mm thickness PVC sheet was larger than the forces which were tested with other thickness PVC sheet (0.35, 0.2, 0.1 mm) and no PVC sheet. Because the numbers of AU which presented the acting force with 0.5 mm thickness PVC sheet were more than numbers of AU in other thickness PVC sheet (0.35, 0.2, 0.1 mm) and no PVC sheet as shown in Fig. 5(c)–(g). But, the 0.5 mm thickness PVC sheet compared other thickness PVC sheet (0.35, 0.2, 0.1 mm), and no PVC sheet cannot contact with the smooth mirror completely well under the same preload.

Therefore, we designed a novel structure of the toe which composed PVC sheet (0.35 mm) and MSAMS. Because PVC sheet (0.35 mm) contacted with the MSAMS on two sides like an arc, the AU will be contact with the surface completely. PVC sheet (0.35 mm) is better, because it was not too hard that it can be rolled from one side like gecko's toe locomotion, and it also was not very soft that it can provide much more normal force.

As shown in Fig. 6, when the angles (θ_1 and θ_2) are very small, the adhesive forces (F_1 and F_2) are very large. We can get the relationship with following equation:

$$\begin{cases} F_1 \sin(\theta_1) + F_2 \sin(\theta_2) = \sum f_y \\ F_1 \cos(\theta_1) + F_2 \cos(\theta_2) = 0 \\ F_y = \sum f_y \end{cases} \quad (1)$$

3.4 Test Analysis and Results of Normal Forces

As shown in Fig. 7, based on the novel structure of the toe which composed PVC sheet (0.35 mm) and MSAMS, we designed three different contact statuses: (I) when the PVC sheet contacted with the MSAMS completely, we marked this status as No Arc; (II) when the PVC sheet contacted with the MSAMS on the two sides, we marked this status as One Arc; and (III) when the PVC sheet contacted with the MSAMS on the middle and two sides, we marked this status as Two Arcs.

The novel toe which actually driven by the motor was pushed by two threads. The different locomotion of threads may affect the performance of adhesive normal

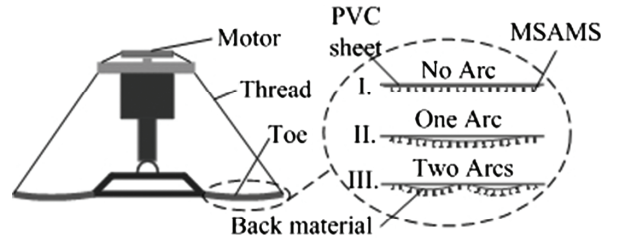


Figure 7. Three contacted statuses between PVC sheet (0.35 mm) and MSAMS: (I) PVC sheet contacted with the MSAMS completely (marked by No Arc); (II) PVC sheet contacted with the MSAMS on the two sides (marked by One Arc); and (III) PVC sheet contacted with the MSAMS on the middle and two sides (marked by Two Arcs).

force. As shown in Fig. 8, we designed three different operating models of the bionic foot. As shown in Fig. 8(a1)–(a4), there was no thread-driven in the model A during all situations. As shown in Fig. 8(b1)–(b4), there was a thread-driven before contact in the model B, but there was no thread-driven in other situations. As shown in Fig. 8(c1)–(c4), there was a thread-driven in the model C during all situations.

We fixed a mirror (the size of 150 mm × 200 mm) on the horizontal surface of the electronic scale and placed with some weights as preload. The coordination was showed in Fig. 9. The bionic foot with dry adhesive material will be contacted with the mirror under different preload. The PVC sheets with 0.35 mm thickness were tied down by eight threads which were driven by a motor.

We defined the direction of the adhesive normal force (F_y) was along the axis y in all the testing experiments. The camera recorded the adhesive normal force (F_y) data on the screen. Each toe was attached with dry adhesive material whose size was 25 mm × 45 mm.

We tested three kinds of structure of toe (No Arc, One Arc and Two Arcs) in Model A. As shown in Fig. 10(a), the 500 and 1,000 g weights were forced on the foot as normal preload. It showed that adhesive normal force of bionic foot with Two Arcs was larger than others. When the preloads were increasing, the adhesive normal forces in Model A were also increasing simultaneously. As the same way, we tested three kinds of structure of toe (No Arc, One Arc and Two Arcs) in Model B as shown in Fig. 10(b). When 500 and 1,000 g weights were forced on the foot as normal preload, the adhesive normal force of bionic foot with Two Arcs was larger than others. Actually, when the preloads were increasing, the adhesive normal forces in Model B were also increasing simultaneously.

As shown in Fig. 10(b), in order to analyze the difference of normal adhesive force with preloads, we selected four kinds of preloads (250, 500, 750 and 1,000 g) and compared the normal adhesive force of bionic foot with Two Arcs in Models A and B. It shows that normal adhesive force of bionic foot with Two Arcs in Model A was larger than the other one in Model B. Especially, the normal adhesive force which was about 7.5 N with 250 g preload in Model B almost approximate to the normal adhesive force with 1,000 g preload in Model A. It is easily to get the

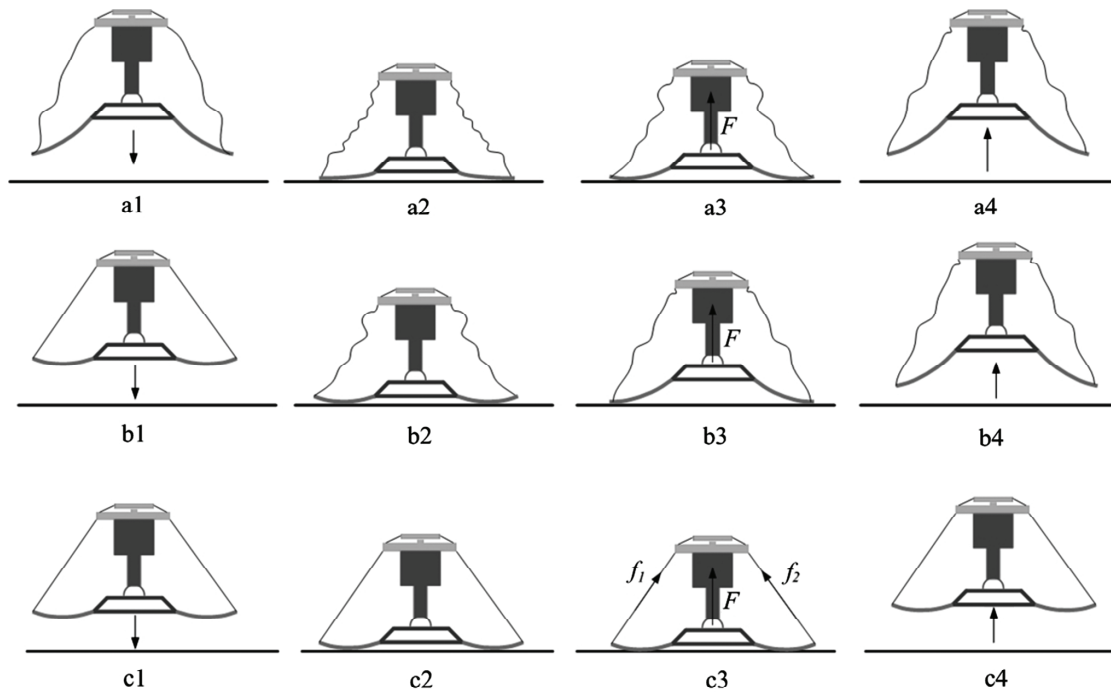


Figure 8. Three different operating models of the bionic foot: (a1) No thread-driven before contact in model A; (a2) after the foot contacts, there is no thread-driven in model A; (a3) when the normal force acted, no thread-driven in model A; (a4) there is no thread-driven during detachment in model A; (b1) thread-driven before contact in model B; (b2) after it contacts, no thread-driven in model B; (b3) when normal force acted, there is no thread-driven in model B; (b4) no thread-driven during detachment in model B; (c1) thread-driven before contact in model C; (c2) thread-driven after contact in model C; (c3) thread-driven when normal force acted in model C; and (c4) thread-driven during detachment in model C.

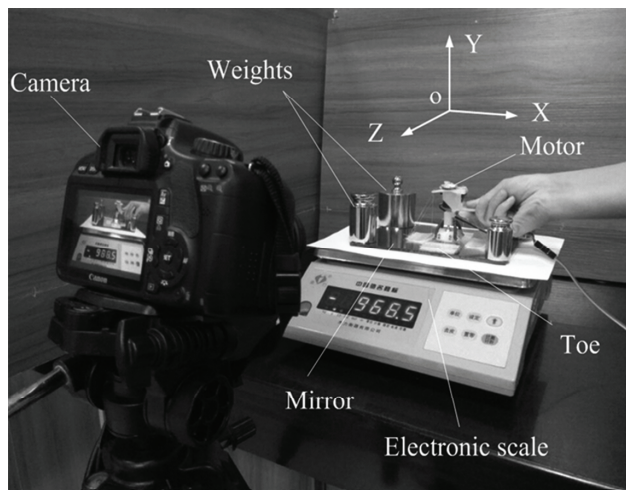


Figure 9. Equipment and methods for testing adhesive normal force.

results that the structure of bionic foot with Two Arcs is better than others, and locomotion of Model B is better than Model A.

We tested three kinds of structure of toe (No Arc, One Arc and Two Arcs) in Model C. As shown in Fig. 11, compared the Model C with the Model B, adhesive normal force of bionic foot with Two Arcs was larger than others.

It is easy to get the results that the structure of bionic foot with Two Arcs is better than others, and locomotion

of Model C is better than Model B. When the preloads were increasing, the adhesive normal forces in Model C were also increasing simultaneously.

If the bionic adhesive foot needs large preloads when it contact with a surface, and the other foot will need much more normal adhesive force in the locomotion of climbing ceiling. We usually selected a kind of structure and locomotion for bionic gecko foot, which had the little preloads and large adhesive normal force. In the same situations with the little preload (250 g), compared the adhesive normal force with different structures, we found that the structure of bionic foot with Two Arcs was about 8.5 N in Model C, and it was better than others.

4. Experiments of Gecko Robot

Based on the testing results of the bionic foot, we use the structure with Two Arcs, and carry on the attached locomotion in Model C. As shown in Fig. 12, the Gecko robot_7 is made by IBSS, and this novel legged Gecko robot has about 700 g weights (with battery), the sizes of 400 mm × 260 mm × 80 mm, 16 active and 12 passive degrees of freedom were designed with four legs for climbing to an inverted flat glass. The foot of Gecko robot_7 was driven actively by a motor and eight threads, and each leg was driven actively by three motors. Actively, Gecko robot_7 can adapt to 3D space in locomotion by principle. We select PVC sheet with 0.35 mm thickness as the substrate of toe and use dry adhesive material with the

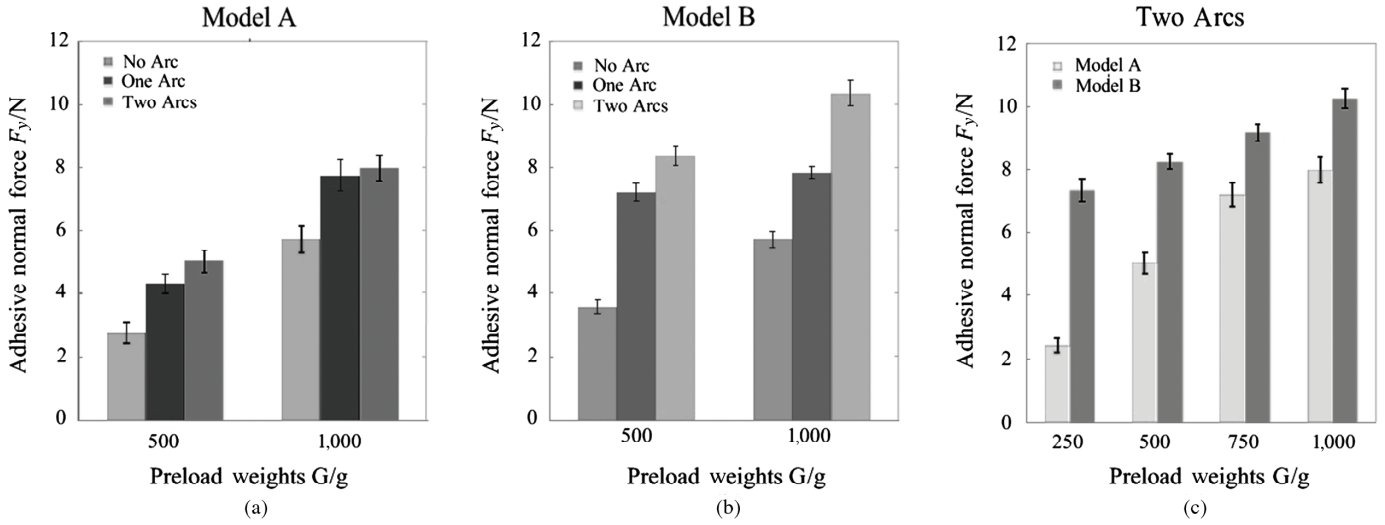


Figure 10. Adhesive normal force of dry adhesive material under different conditions: (a) No Arc, one Arc and two Arcs with Model A; (b) No Arc, one Arc and two Arcs with Model B; and (c) Two Arcs with Models A and B.

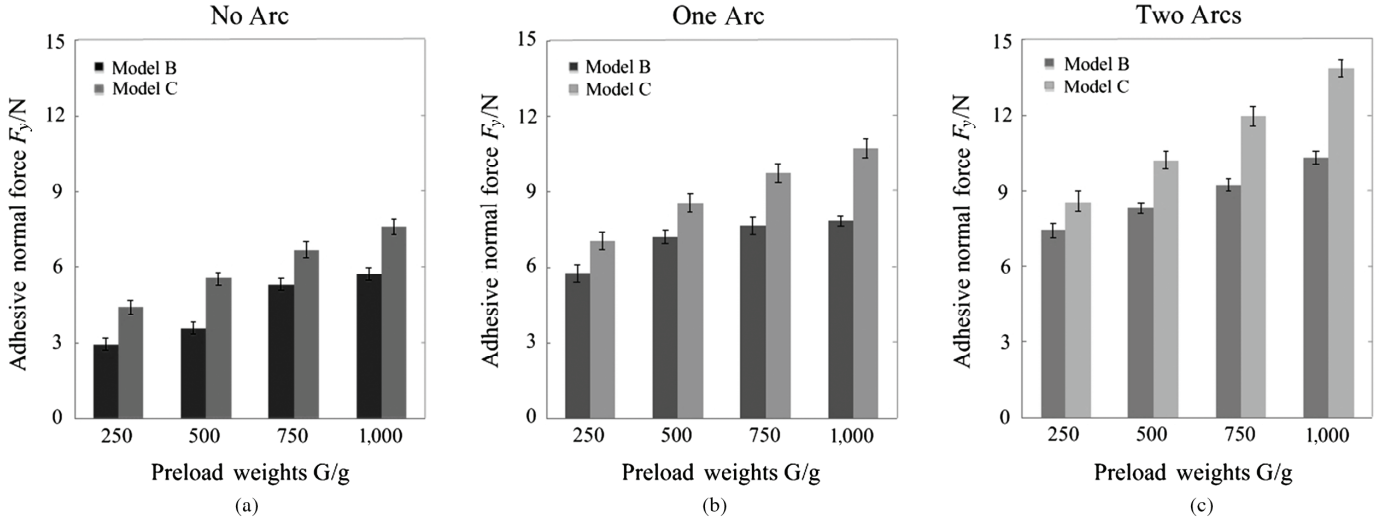


Figure 11. Adhesive normal force of dry adhesive material under different conditions: (a) No Arc with Models B and C; (b) One Arc with Models B and C; and (c) Two Arcs with Models B and C.

size of 45 mm \times 25 mm in each toe. During the climbing ceiling locomotion, the contact forces can be recorded by a 3-dimension force sensor in foot. During the experiments of the ceiling locomotion, some actual control methods in tracking were referenced from these papers [28], [29].

Figure 13 shows the different situations in one circle of climbing ceiling locomotion of Gecko robot_7. We use diagonal gait with 50 mm stride. It climbs the inverted glass surface (180°) in 30 s for one circle. There are first and second half circle because of the diagonal gait.

Figure 14 shows the adhesive normal forces during the climbing ceiling locomotion. Because Gecko robot_7 climbs on the ceiling slowly, we can ignore the effect of inertia forces. When the summation of normal forces (F_{1y} , F_{2y} , F_{3y} , F_{4y}) overcomes the weight (G) of Gecko robot_7, the climbing ceiling locomotion may be successful. Specially, in the situation C, when the bionic adhesive foot contact with the surface, there are contacted normal forces (F_{2y} , F_{3y}), which are opposite to the adhesive normal

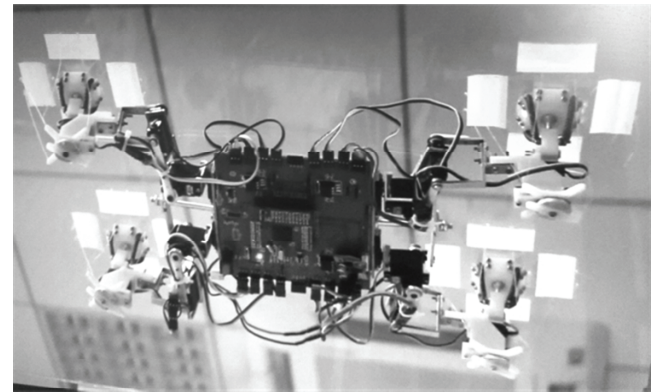


Figure 12. Gecko robot_7.

forces (F_{1y} , F_{4y}). The same things happen in situation F. If the contacted normal forces (F_{2y} , F_{3y}) as preloads are large, we need larger adhesive forces (F_{1y} , F_{4y}) because of the gecko robot's balance of forces. The climbing

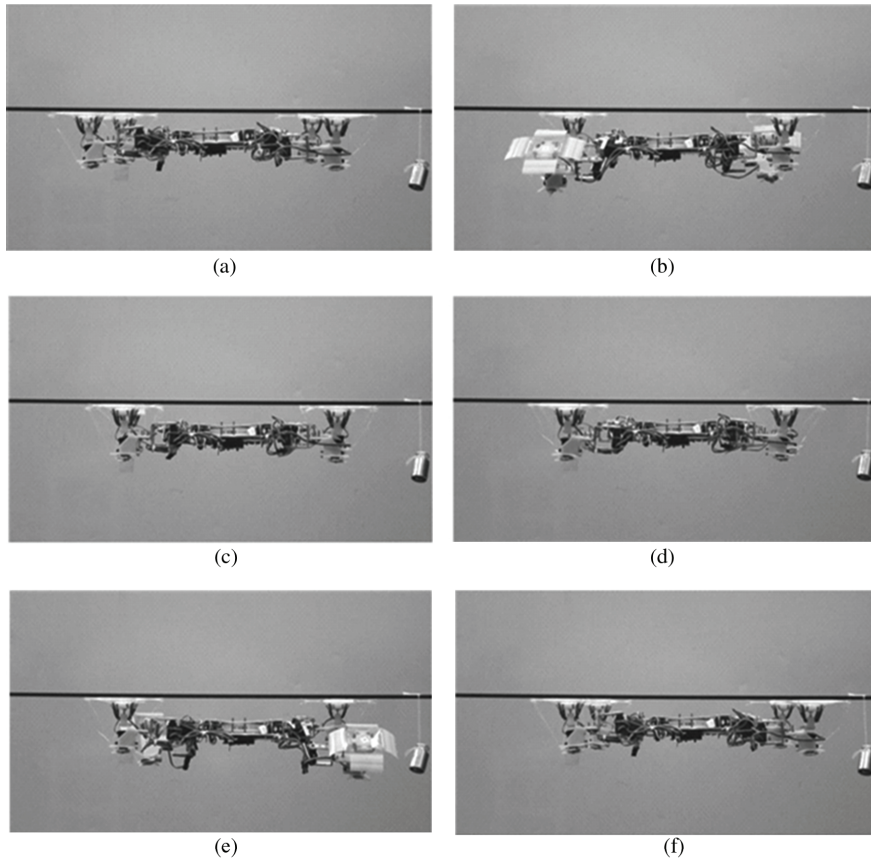


Figure 13. Different situations in one circle of climbing ceiling locomotion of Gecko robot_7: (A) Four legs attached on the surface in first half circle; (B) two legs attached on the surface and two legs peeled off the surface in first half circle; (C) two legs attached on the surface and two legs pushed the surface in first half circle; (D) four legs attached on the surface in second half circle; (E) two legs attached on the surface and two legs peeled off the surface in second half circle; and (F) two legs attached on the surface and two legs pushed the surface in second half circle.

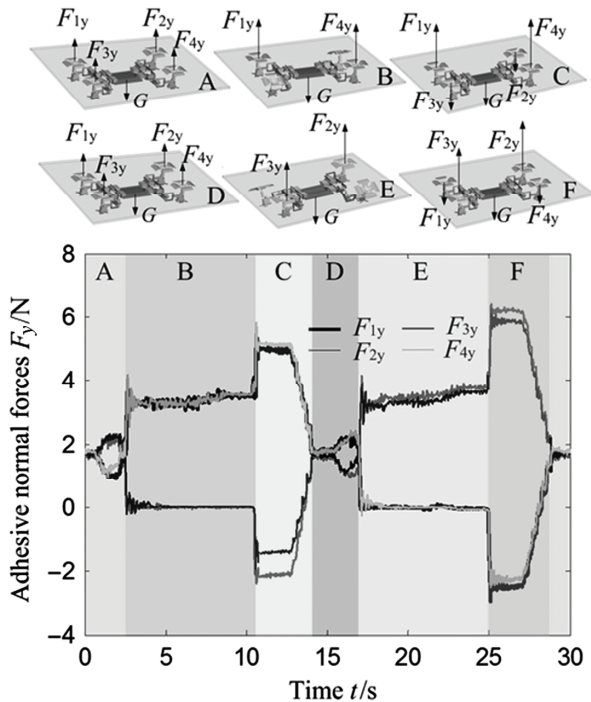


Figure 14. The adhesive normal forces during the climbing ceiling locomotion.

ceiling experiment shows that the bionic gecko foot with the structure of Two Arcs and the locomotion of Model C is applied in the Gecko robot_7 successfully. It is the first time to carry on the climbing ceiling experiment of legged gecko robot successfully by using dry adhesive material PVS.

5. Conclusion

In this paper, we design the structures of bionic adhesive gecko foot by studying the gecko's locomotion and analyse many more different factors which influence adhesion performance. We can get some conclusions as following: (1) the normal adhesive force and size of contact areas have linearity relationship obviously; (2) the soft substrate contributes to increase the contact areas and helps bio-gecko toes to contact with target surface completely; and (3) the structure of bionic foot with Two Arcs is better than others, and locomotion of Model C is better than Models B and A. Bionic gecko robot with the novel adhesive foot climbed the ceiling smooth surface stably, and it showed the rationality and feasibility of the bionic foot structure design.

Acknowledgement

This article is supported by the National Natural Science Foundation of China (Grant No. 51475230, 51105201, 51435008) and the Fundamental Research Funds for the Central Universities (Grant No. 3082018NT2018022, kfjj20171504). We thank Gorb for providing some testing data and papers. We thank all the reviewers for their suggestions.

References

- [1] K. Autumn, Y.A. Liang, S.T. Hsieh, W. Zesch, *et al.*, Adhesive force of a single gecko foot-hair, *Nature*, 405, 2000, 681–685.
- [2] K. Autumn, A.M. Peattie, Mechanisms of adhesion in geckos, *Integrative and Comparative Biology*, 42, 2002, 1081–1090.
- [3] K. Autumn, S.T. Hsieh, D.M. Dudek, *et al.*, Dynamics of geckos running vertically, *Journal of Experimental Biology*, 209(2), 2006, 260–272.
- [4] Y. Tian, D. Tao, N. Pesika, *et al.*, Flexible control and coupling of adhesion and friction of gecko setal array during sliding, *Tribology Online*, 10(2), 2015, 106–114.
- [5] Z. Wang, L. Cai, W. Li, *et al.*, Effect of slope degree on the lateral bending in gekko geckos, *Journal of Bionic Engineering*, 12(2), 2015, 238–249.
- [6] Z. Wang, Z. Dai, A. Ji, *et al.*, Biomechanics of gecko locomotion: The patterns of reaction forces on inverted, vertical and horizontal substrates, *Bioinspiration & Biomimetics*, 10(1), 2015, 1–14.
- [7] Z. Wang, Z. Dai, W. Li, *et al.*, How do the substrate reaction forces acting on a gecko's limbs respond to inclines, *The Science of Nature*, 102(1–2), 2015, 1–15.
- [8] A. Ji, C. Ge, H. Wang, *et al.*, Adhesion of gecko on vertical surfaces with different roughness, *Chinese Science Bulletin*, 61(23), 2016, 2578–2586.
- [9] M.P. Murphy, B. Aksak, M. Sitti, Gecko-inspired directional and controllable adhesion, *Small*, 5(2), 2009, 170–175.
- [10] S. Das, N. Cadirov, S. Chary, Y. Kaufman, *et al.*, Stick-slip friction of gecko-mimetic flaps on smooth and rough surfaces, *Journal of the Royal Society Interface*, 12(104), 2015, 1–9.
- [11] M. Varenberg, S. Gorb, Shearing of fibrillar adhesive microstructure: friction and shear-related changes in pull-off force, *Journal of the Royal Society Interface*, 4(15), 2007, 721–725.
- [12] G.D. Wile, K.A. Daltorio, L.R. Palmer, *et al.*, Making orthogonal transitions with climbing Mini-WhegsTM, *IEEE International Conf. on Robotics and Automation*, Pasadena, California, USA, 2008, 1775–1776.
- [13] X. Wu, D. Wang, A. Zhao, D. Li, *et al.*, A wall-climbing robot with biomimetic adhesive pedrail, *Advanced Mechatronics and MEMS Devices*, Springer, New York, 2013, 179–191.
- [14] T.W. Seo, M. Sitti, Tank-like module-based climbing robot using passive compliant joints, *IEEE/ASME Transactions on Mechatronics*, 18(1), 2013, 397–408.
- [15] K.H. Koh, M. Sree Kumar, S.G. Ponnambalam, Feasibility study for applying electrostatic adhesion on wall climbing robots, *International Journal of Advancements in Mechanical and Aeronautical Engineering*, 1(4), 2014, 53–58.
- [16] O. Unver, A. Uneri, A. Aydemir, M. Sitti, Geckobot: A gecko inspired climbing robot using elastomer adhesives, *Proc. IEEE International Conf. on Robotics and Automation*, Orlando, Florida, USA, 2006, 2329–2335.
- [17] P. Birkmeyer, A.G. Gillies, R.S. Fearing, Dynamic climbing of near-vertical smooth surfaces, the *IEEE/RSJ International Conf. on Intelligent Robots and Systems*, Vilamoura, Algarve, Portugal, 2012, 286–292.
- [18] S. Kim, M. Spenko, S. Trujillo, *et al.*, Smooth vertical surface climbing with directional adhesion, *IEEE Transactions on Robotics*, 24(1), 2008, 65–74.
- [19] Z. Yu, B. Yang, S.X. Yang, *et al.*, Vertical climbing locomotion of a new gecko robot using dry adhesive material, *International Journal of Robotics and Automation*, 32(4), 2017, 425–431.
- [20] Z. Yu, Z. Wang, R. Liu, *et al.*, Stable gait planning for a gecko-inspired robot to climb on vertical surface, *IEEE International Conf. on Mechatronics and Automation*, Takamatsu, Kagawa, Japan, 2013, 307–311.
- [21] O. Unver, M. Sitti, A miniature ceiling walking robot with flat tacky elastomeric footpads, *IEEE International Conf. on Robotics and Automation*, Kobe, Japan, 2009, 2276–2281.
- [22] O. Unver, M. Sitti, Tankbot: A miniature, peeling based climber on rough and smooth surfaces, *Robotics and Automation*, *IEEE International Conf. on Robotics and Automation*, Kobe, Japan, 2009, 2282–2287.
- [23] O. Unver, M. Sitti, Tankbot: A palm-size, tank-like climbing robot using soft elastomer adhesive treads, *The International Journal of Robotics Research*, 29(14), 2010, 1761–1777.
- [24] W.A. Breckwoldt, K.A. Daltorio, L. Heepe, *et al.*, Walking inverted on ceilings with wheel-legs and micro-structured adhesives, *IEEE/RSJ International Conf. on Intelligent Robots and Systems*, Hamburg, Germany, 2015, 3308–3313.
- [25] H. Ko, H. Yi, H.E. Jeong, Wall and ceiling climbing quadruped robot with superior water repellency manufactured using 3D printing (UNIClimb), *International Journal of Precision Engineering and Manufacturing-Green Technology*, 4(3), 2017, 273–280.
- [26] A.E. Kovalev, M. Varenberg, S.N. Gorb, Wet versus dry adhesion of biomimetic mushroom-shaped microstructures, *Soft Matter*, 8(29), 2012, 7560–7566.
- [27] L. Heepe, M. Varenberg, Y. Itovich, *et al.*, Suction component in adhesion of mushroom-shaped microstructure, *Journal of the Royal Society Interface*, 8, 2011, 585–589.
- [28] A. Zhu, S.X. Yang, Tracking control of a mobile robot with stability analysis, *International Journal of Robotics and Automation*, 28(4), 2013, 340–348.
- [29] S.X. Yang, A. Zhu, M.Q.H. Meng, *et al.*, A bioinspired neurodynamics-based approach to tracking control of mobile robots, *IEEE Transactions on Industrial Electronics*, 59(8), 2012, 3211–3220.

Biographies



Zhiwei Yu received his Ph.D. degree in the College of Mechanical and Electrical Engineering from Harbin Engineering University, Harbin, China, in 2008. Currently, he is an Associate Professor of College of Astronautics at Nanjing University of Aeronautics and Astronautics, Nanjing, China. He was a Visiting Professor in the Advanced Robotics and Intelligent Systems (ARIS)

Laboratory at the University of Guelph in Canada from December 2014 to January 2016. He has published over 30 papers in the related international conferences and journals. His research interests include bio-inspired robots, legged robots, locomotion control and intelligent systems.



Ye Shi received her bachelor degree in automation from the Nanhang Jincheng College, Nanjing, China, in 2015. Currently, she is a postgraduate in the College of Astronautics at Nanjing University of Aeronautics and Astronautics, Nanjing, China. Her research interest is locomotion of gecko robot.



Jiaxing Xie received his bachelor degree in automation from Nanjing University of Aeronautics and Astronautics, Nanjing, China, in 2015. Currently, he is a postgraduate in College of Astronautics at Nanjing University of Aeronautics and Astronautics, Nanjing, China. His research interests include legged robot and locomotion control.



Zhendong Dai received his Ph.D. degree in College of Mechanical and Electrical Engineering from Nanjing University of Aeronautics and Astronautics, Nanjing, China, in 2000. Currently, he is a Professor and the Head of Institute of Bio-inspired Structure and Surface Engineering (IBSS) at Nanjing University of Aeronautics and Astronautics, Nanjing, China. He has published over 200 papers in the related international conferences and journals. His research interests include bio-inspired systems, robotics, bionic structure and material, multi-sensors, tribology and neurobiology.



Simon X. Yang received the B.Sc. degree in engineering physics from Beijing University, China, in 1987, the first of two M.Sc. degrees in biophysics from Chinese Academy of Sciences, Beijing, China, in 1990, the second M.Sc. degree in electrical engineering from the University of Houston, USA, in 1996, and the Ph.D. degree in electrical and computer engineering from the

University of Alberta, Edmonton, Canada in 1999. He joined the School of Engineering at the University of Guelph, Canada, in 1999. Currently, he is a Professor and the Head of the Advanced Robotics and Intelligent Systems (ARIS) Laboratory at the University of Guelph in Canada. His research interests include intelligent systems, robotics, sensors and multi-sensor fusion, wireless sensor networks, control systems, soft computing and computational neuroscience.